Performance of a polypropylene membrane contactor for the recovery of dissolved methane from anaerobic effluents: mass transfer evaluation, long-term operation and cleaning strategies

Journal of Membrane Science, Volume 563, 1 October 2018, Pages 926-937

https://doi.org/10.1016/j.memsci.2018.06.045

(María) Henares, (Pablo) Ferrero, (Pau) San-Valero, (Vicente) Martínez-Soria, (Marta) Izquierdo*

Research Group GI^{2}AM, Department of Chemical Engineering, University of Valencia, Avda. Universitat s/n, 46100 Burjassot, Spain

*Corresponding author: E-mail address: marta.izquierdo-sanchis@uv.es (M. Izquierdo)

URL: http://giam.blogs.uv.es/

Abstract

A polypropylene membrane contactor was used for the recovery of dissolved methane from an anaerobic reactor effluent. Effect of operational parameters, operation mode and fouling on long-term operation was studied using vacuum pressure or N_2 as sweep gas. Results were analyzed based on the mass transfer estimations. Lower performance was observed in the shell-side mode due to the lower liquid velocity and the probable channeling. Membrane pore wetting was observed with the increase in Q_L in the vacuum-pressure mode. This was confirmed with mass transfer resistance analysis, resulting in an estimated wetted pore fraction of between 0.25 and 0.53. The highest removal efficiencies were obtained with the liquid flowing in the lumen side and sweep-gas operation (between 98% and 67% for Q_L between 4.1 and 27.2 L h^{-1}), with negligible effect of the N_2 flow rate. In the long-term operation, the impact of membrane fouling was less intense in the lumen side, with longer operation time and more reversible fouling. A complete characterization of the fouling based on water sample analysis concluded that both inorganic and organic foulants were present, probably with higher biofouling presence. A combination of water and chemical cleanings resulted in a recommended protocol based on daily water cleaning.

Keywords

Anaerobic reactor; fouling; mass transfer; membrane contactor; methane degassing

1. Introduction

Anaerobic reactors for the wastewater treatments generate a methane-rich biogas, which can be used in combustion for the production of heat and/or electricity. Even though the low solubility of methane in water, residual dissolved methane (D-CH_4) is often present in the final water effluent, especially in anaerobic treatments at sub-mesophilic and psychrophilic temperatures (<25 ºC) due to the increase in gas solubility at low temperatures [1]. Increase in greenhouse gas diffuse emissions, loss of energy source and generation of potential explosive atmospheres when discharged into closed vessels or sewers are the main problems when managing these effluents. Thus, its recovery/removal is necessary for economic, environmental and security reasons. The treatment technologies for gas desorption from anaerobic waters include spray aeration, packed towers, tray aerators, diffuse aeration, and membrane contactors [2]. The use of membrane contactors is a commercially available mature technology for applications such as O_2 or CO_2 removal, among others [3]. However, its application for the removal D-CH_4 from anaerobic effluents is still at research/pilot level. From the first promising results [4-8] , the number of published papers has grown in recent years [9-14], demonstrating the interest of scientific community in this technology. However, some practical implications, such as the long-term stability of membrane contactors and the optimum driving force (vacuum/sweep gas) are still scarcely studied, and further research is needed.

Membrane contactors offer many advantages over conventional technologies [2]; however, the presence of the membrane introduces an additional mass transfer resistance. Depending on membrane material, the nature of the liquid phase and transmembrane pressure, the membrane pores may be occupied by liquid, corresponding to the so-called wetted operation, which strongly decreases the permeate flux. Measures to prevent the wetting problem may include the increase in the hydrophobicity of the membrane by increasing the contact angle between the liquid and the membrane [14]. The surface tension of the liquid phase also plays an important role. The presence of organic compounds may decrease the surface tension of solutions, which decreases the breakthrough pressure, leading to a rapid increase in membrane wetting. The wetting phenomenon is an effect widely studied in the CO_2 absorption using organic absorbents [15,16], and water-based absorbents [17-19]. In the application of membrane contactors for degassing water solutions, the wetting phenomenon is also reported to be associated with the increase in liquid flow rate [10,20].

The driving force for D-CH_4 removal can be obtained by applying vacuum or using a sweep gas on the gas side. For the recovery and reuse of the downstream gas phase, methane concentration in the recovered gas for commercial microturbines should be higher than 35% [21]. To achieve such a concentration, sweep-gas mode at low gas-to-liquid flow-rate ratio (G/L) was proposed [11]; however, this induced an increase in gas phase mass transfer resistance, and so a reduction in the D-CH_4 recovery efficiency. Vacuum operation overcomes this problem and some authors recommend it [12,22]. However, vacuum operation is less energetically favorable than use of sweep gas, and higher pressure difference between gas and liquid phase could induce pore wetting [10].

Loss of performance due to membrane fouling is one of the main problems encountered when coupling biological reactors and membrane technologies. In this regard, natural organic matter related to microbial and extracellular polymer substances has been described as the major type of foulant in biological wastewater treatment units [23]. Fortunately, membrane contactors are less sensitive to fouling, since there is no convective flow through the membrane pores causing

concentration polarization, as in the pressure-driven membrane process of membrane bioreactors. Clogging due to suspended particles coming from the regular discharge of surplus biomass particles may be a major concern in membrane contactors, and prefiltration is necessary. Suspended solid concentration in anaerobic effluents usually are in the range 100 – 300 mg L^{-1}. The particle size analysis of the effluent of a laboratory-scale anaerobic reactor operated under similar conditions than the one of this study revealed that 60-85% of solids were higher than 300 μm, so susceptible of generate rapid clogging of the hollow fiber membrane contactors, especially when liquid flows inside the fibers [24]. Also, protein adsorption (organic fouling) and salt precipitation (inorganic fouling) onto the membrane surface can be involved as causes of fouling [25,26]. For the industrial application of the technology, operational and cleaning strategies optimization are of crucial interest for the prevention of the use of cleaning chemicals to ensure an economically feasible operation with a long stable life of the system.

Few studies can be found in the literature that evaluate the long-term operation of membrane contactors for methane degassing. Bandara et al. [5,6] indicated that membrane fouling of the contactor was insignificant for their long-term experiments with a lab-scale UASB reactor (>30days). Sethunga et al. [14] operated a modified PVDF hollow fiber membrane contactor with synthetic water containing dissolved biogas for 10 days to investigate the resistance to pore wetting, and concluded that the fluctuation of the methane flux was less than 10%. In our previous work [12] with a PDMS membrane contactor, long-term experiments in lumen-side and shell-side mode treating an anaerobic effluent included both intermediate water and chemical cleaning and the characterization of organic and inorganic foulants. Results highlighted the importance of implementing a prevention strategy of membrane fouling, based preferably on the use of water cleaning. The polypropylene membrane contactor of this study showed higher removal efficiency than the PDMS in short-term experiments when pore wetting phenomenon was not observed [10]. For the industrial application of the technology, it is crucial not only the short-term efficiency but also the performance in long-term and continuous operation, so the present work extend and complement our previous studies and allow comparison of response of membrane materials from the fouling perspective.

In this context, the aim of this work is to assess the performance of a polypropylene membrane contactor for the removal of dissolved methane from the effluent of a laboratory-scale expanded granular sludge-bed anaerobic reactor. Influence of the operational parameters (liquid flow rate, vacuum pressure and sweep gas flow rate) on the methane removal efficiency was studied in short-term experiments. An analysis of the results based on mass transfer evaluation is also presented. In the present work, our previous study [10] is broadened, with a greater range of operation conditions, including an estimation of the mass transfer resistances with literature correlations. As a special novelty, to study the impact of the fouling on removal efficiency, long-term experiments in the lumen side and shell side were performed. Research efforts were aimed at characterizing the fouling and optimizing the cleaning strategies, focusing on the application of the technology.

2. Materials and methods

2.1.Experimental set-up and operation

The anaerobic effluent used in the degassing experiments came from a laboratory-scale expanded granular sludge-bed (EGSB) anaerobic reactor operated at 25 ºC. Granular anaerobic sludge (4 L) from the wastewater treatment plant of a local brewery (Font Salem, El Puig) was used for inoculation. The reactor treated 8 L d^{-1} of synthetic wastewater polluted with ethanol

with an organic load rate of 30 kg chemical oxygen demand (COD) m^{-3} d^{-1}. The sludge bed was kept expanded with a recirculation up-flow velocity of 10.7 m h^{-1}. A liquid–gas separator device was placed at the top of the reactor. The gas outlet was connected to a gas wash bottle containing sodium hydroxide solution to remove carbon dioxide and hydrogen sulfide from the biogas. Biogas composition of the headspace of the bioreactor was measured from samples taken prior to the gas wash bottle. The methane flow rate was monitored periodically with a gas flowmeter (MGC-10 PMMA, Ritter, Germany) and the pH and conductivity with a multiparameter sensor (pH/Cond 340i WTW, Germany). Alkalinity, volatile fatty acids (VFA), COD, and nutrient concentration in the inlet and outlet of the reactor were analyzed according to standard methods [27]. A detailed description of the system and procedure can be found elsewhere [28,29].

A commercial hollow-fiber membrane contactor with polypropylene (PP) fibers was used for D-CH_4 removal (1×5.5 MiniModule, Liqui-Cel, Membrana GmbH, Germany), connected to the recirculation stream of the bioreactor, with similar composition to the final effluent. The main characteristics of the membrane contactor are presented in Table 1. The anaerobic stream was pumped through the contactor using a peristaltic pump (Watson-Marlow, USA). A 40 µm prefilter was placed prior to the contactor, in order to prevent the membrane contactor clogging with particulate matter from the bioreactor. Liquid pressures at the inlet and outlet of the membrane contactor were measured using a portable manometer MP112 (Kimo, Spain). A complete scheme of the EGSB reactor and the membrane contactor is presented in Figure 1.

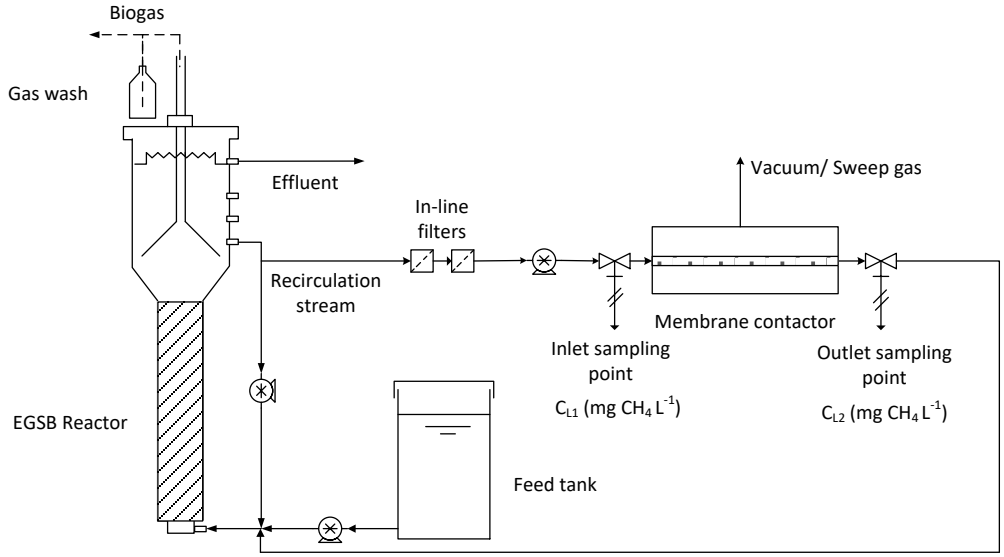

Figure 1. Scheme of the set-up of the EGSB reactor and degassing membrane contactor

Table 1. Polypropylene membrane contactor specifications and operational conditions.

Module inner diameter, m	0.025
Module length, m	0.176
Number of fibres	2300
Effective fibre length, L, m	0.1397
Inner diameter, μm	220
Outer diameter, μm	300
Fibre wall thickness, l, μm	40
Inner area, A_i, m^2	0.180
Outer area, A_o, m^2	0.303
Pore radius, r_p, μm	0.02
Shell inner diameter, m	0.025
Packing fraction, ϕ	0.33
Porosity, ε	0.4
Tortuosity, τ	1.4
Lumen side volume, m^3	16×10^{-6}
Shell side volume, m^3	25×10^{-6}
Max. liquid flow-rate, Q_L, L h^{-1}	30
Typical sweep gas flow-rate, Q_{N2}, L h^{-1}	26.0-800

2.2. Operation of the membrane contactor

Comparison of the main parameters affecting the performance of the contactor was carried out in 39 short-term experiments of around 90 min, the minimum time necessary to assure stable operation [10]. In this previous work [10], some performance results of these short-term experiments were used, in order to compare a PDMS (nonporous) and a PP (porous) membrane contactor for D-CH_4 removal. We have broadened the study to delve into the effect of the operational conditions on the PP contactor performance. A total of 20 vacuum pressure experiments (vacuum pump N026.3.AT.18, KNF Neuberger, Germany) were carried out with vacuum pressures of –140, –500 and –800 mbar, with the liquid flowing through the lumen (Lumen-Side mode, LS) and through the shell (Shell-Side mode, SS). Likewise, a total of 19 countercurrent sweep-gas experiments were carried out using high purity N_2 (>99.8%, Carburos Metálicos, SA). Sweep-gas flow was fixed in the range 26–800 L N_2 h^{-1}, and it was introduced using a mass flow controller (Bronkhorst Hi-Tec, The Netherlands). Both in the vacuum and in the sweep-gas experiments, liquid flow was also varied between 4.1 and 27.2 L h^{-1}. Operational conditions were fixed in the range of values recommended by the supplier in order to elucidate their effect on the D-CH_4 removal efficiency. Performance of the contactor was evaluated by analyzing D-CH_4 in water samples at the inlet (C_{L1}, mg L^{-1}) and outlet (C_{L2}, mg L^{-1}) of the module at the end of the experiment, and the removal efficiency (RE,%) was calculated:

$$RE = \frac{C_{L1} - C_{L2}}{C_{L1}} \times 100 \quad (1)$$

During the short-term experiments, a daily cleaning with deionized water in countercurrent flow was applied for 30 min. Likewise, a control experiment was repeated periodically to check that the RE was not altered over the whole period, accounting for 3510 h of operation in LS mode and 1620 h in SS mode without loss of efficiency due to fouling.

Fouling of the membranes is one of the main operational problems that membrane technologies must face. In order to evaluate the response of the system to continuous operation, two long-term experiments were carried out with N_2 flow rate of 26 L h^{-1} as sweep gas: one with the liquid through the lumen and another through the shell, with a liquid flow rate of 20.4 L h^{-1}. Follow-up of the performance was carried out by analyzing the D-CH_4 every 2–3 h of operation. Water and N_2 flow rates were checked daily. Cleaning of the contactor was performed only when RE decreased. Two different cleaning protocols were used: (1) countercurrent deionized water cleaning for 2 h, as a soft conventional protocol; (2) a chemical cleaning applied when the water cleaning was ineffective. The chemical cleaning used, recommended by the supplier [30], consisted first of a countercurrent flow of a 2% (w/w) sodium hydroxide solution for 2 h in a closed loop, then a water cleaning for 10 min, followed by a flow of 10% (w/w) citric acid solution for 2 h in closed loop, and a final water cleaning for 10 min. Solutions resulting from the chemical cleaning were analyzed to characterize the nature of the fouling and to optimize the cleaning protocol.

The presence of biofouling was elucidated with an experiment consisting of flowing 250 mL of a solution that mimicked the feed of the anaerobic reactor through the membrane contactor in a closed loop for 4 h at 20 L h^{-1}, without application of vacuum pressure or sweep gas. The solution was composed of 800 mg COD/L of ethanol, with alkalinity and macro- and micro-nutrients according to Lafita et al. [27]. The COD concentration of the feed solution was analyzed at the beginning and end of the experiment. The experiment was performed when the membrane was fouled, and a blank test (cleaned membrane) was carried out for comparison purposes.

2.3. Sampling and analytical methods

Water samples were taken from the recirculation of the bioreactor (before the 40 μm prefilter), from the inlet (after filtration) and from the outlet of the membrane contactor with a three-way valve system. A complete characterization of water samples was performed to determine the D-CH_4 removal efficiency and to evaluate the change of the water quality and its potential influence on the fouling appearance and mechanisms.

D-CH_4 was determined using a headspace method as described elsewhere [12]. Briefly, 50 mL of water were shaken in a closed vial of 125 mL for 3 h at 25 ºC. After equilibration, the headspace gas concentration (C_{GH}, mg L^{-1}) was analyzed by gas chromatography (Agilent GC 7820A, Spain). The D-CH_4 in liquid phase (C_L, mg L^{-1}) was calculated as:

$$C_L = \frac{C_{GH}\left(V_{GH} + {V_L}/{H}\right)}{V_L} \quad (2)$$

where V_{GH} is the headspace gas volume, V_L is the liquid volume, and H is the dimensionless Henry's law constant (defined as gas per liquid concentration, $C_{GH} = H \cdot C_L$).

Soluble COD and solid content of water samples were determined according to the Standard Methods for the Examination of Water and Wastewater [26]. Soluble Total Organic Carbon (TOC) in water was measured using a total organic carbon analyzer (TOC−VCSH, Shimadzu Corporation, Japan). VFA and alkalinity of centrifuged samples were determined according to the 5-point acid-base titration method, using a potentiometer titrator (848 Titrino Plus, Metrohm, Switzerland). Turbidity of water samples was determined using a turbidimeter according to EN ISO 7027 (Turbiquant® 1500 IT/T, Merck, Germany). pH and conductivity of

liquid samples was measured (pH/Cond 340i WTW, Germany). Concentration of different cations (Ca^{2+}, Mg^{2+}, NH_4^+, Na^+, and K^+) and anions (SO_4^{2-}, NO_3^-, PO_4^{3-}, Cl^-) in liquid samples were measured with an ionic chromatograph (883 Basic IC Plus, Metrohm, Switzerland) equipped with Metrosep C4–250/4.0 and Metrosep A Supp 3 columns. The soluble content of polysaccharides and proteins of water samples were determined by the colorimetric methods proposed by Dubois et al. [31] and Lowry et al. [32], respectively. Biogas production was determined using a biogas volumetric measuring device (MGC-10 PMMA, Ritter, Germany), and biogas composition using a gas chromatograph (Agilent GC 7820A, Spain).

2.4. Mass transfer calculations

The experimental overall mass transfer coefficient (K_{Lexp}, m s^{-1}) of methane was calculated from the mass balance applied at the liquid phase in the membrane contactor by the following differential expression [33]:

$$Q_L \frac{dC}{dA} = -K_{Lexp}(C_L - C_L^*) \quad (3)$$

where Q_L is the liquid flow rate (m^3 s^{-1}), A is the interfacial area (m^2), and C_L^* is the concentration of methane in the liquid phase (mg L^{-1}) in equilibrium with the gas phase calculated from Henry's law ($C_L^* = C_G/H$).

Integration of equation (3) through the membrane contactor (1:inlet, 2: outlet) results in:

$$K_{Lexp} = -\frac{Q_L}{A} ln\left(\frac{C_{L2} - C_L^*}{C_{L1} - C_L^*}\right) \quad (4)$$

The overall mass transfer resistance (R_{ov}, s m^{-3}) is expressed as the sum of the three individual resistances in series in the system: the liquid, membrane and gas mass transfer resistances (R_L, R_m and R_G, respectively). A schematic of the mass transfer resistances for the membrane contactor in gas desorption is included in Appendix A. For the driving force based on the aqueous phase concentration [33]:

$$R_{ov} = \frac{1}{K_L A_L} = \frac{1}{k_L A_L} + \frac{1}{H\ k_m A_{ml}} + \frac{1}{H\ k_G A_G} = R_L + R_m + R_G \quad (5)$$

where K_L is the overall mass transfer coefficient based on liquid driving force (m s^{-1}), k_L, k_m and k_G the individual mass transfer coefficients of the liquid, membrane and gas (m s^{-1}), respectively, A_L the membrane surface in contact with the liquid (0.222 m^2 for lumen-side liquid flow and 0.303 m^2 for shell-side liquid flow), A_{ml} the logarithmic mean membrane surface based on a cylindrical body (0.260 m^2), A_G the membrane surface in contact with the gas (m^2), and H the equilibrium partition coefficient of the solute gas in between the gas and liquid phases (Henry coefficient).

Individual mass transfer coefficients can be estimated using correlations in the form:

$$Sh\ \alpha\ Re^{\alpha}\ Sc^{\beta}\ Gz^{\gamma}\ f(geometry)$$

where *Sh*, *Re*, *Sc* and *Gz* are the Sherwood, Reynolds, Schmidt and Graetz numbers, respectively, and f is a function of the geometry. Table 2 summarizes the equations used in this study for the estimation of the mass transfer coefficients, which are among the most common correlations used for the estimation of coefficients of the fluids (liquid or gas) flowing in the lumen or shell side of a hollow-fiber membrane contactor [33].

When fluid flows through the lumen side, the Lévêque solution (equation 11) [34] was considered for the estimation of coefficients. In contrast to the lumen-side flow, shell-side flow is not fully understood. A number of correlations can be found in the literature, but none is applicable to a wide range of systems as is the Lévêque equation [33]. For the coefficient of the fluid in the shell side in parallel flow, two correlations are considered in this study. Equation 13 was proposed by Prasad and Sirkar [35], and it includes the packing fraction of the contactor. Equation 15 was proposed by Dahuron and Cussler [36], and it is characterized by a Reynolds number exponent deviating from the expected value of 0.6, maybe due to the different channeling around the fibers, according to the authors.

The mass transfer coefficient of the membrane (k_m, m s^{-1}) was estimated by considering the effective diffusion of the transferred species in the gas phase ($D_{G,eff}$, m^2 s^{-1}) [37,38], which is calculated by considering the two types of diffusion distinguished in the porous structure: molecular diffusion ($D_{G,m}$, m^2 s^{-1}) and Knudsen diffusion ($D_{G,Kn}$, m^2 s^{-1}) (equations 16 to 19). Molecular diffusion is determined by the interactions of the molecules [39], and Knudsen diffusion by the interactions of molecules with the pore walls, which become significant for small pores ($d < 0.1$ μm) [40]. Values of the diffusion coefficients of methane in water, nitrogen and air used in this study are summarized in Table 3.

Table 2. Literature correlations for the estimation of the mass transfer coefficients in a porous membrane (k_m), and in the liquid or gas phase (k_L or k_G) when flowing in the lumen or shell side of a hollow-fiber membrane contactor.

Dimensionless numbers			
Sherwood number, *Sh*	$Sh = \frac{k\,d}{D}$	(6)	*d*: fibre diameter, m d_e: equivalent diameter, m *D*: diffusion coefficient in the liquid or gas phase, $m^2\ s^{-1}$ $D_{G,eff}$: effective diffusion of the transferred specie in the gas phase, $m^2\ s^{-1}$ $D_{G,Kn}$: Knudsen diffusion, $m^2\ s^{-1}$ $D_{G,m}$: molecular diffusion, $m^2\ s^{-1}$ *k*: individual mass transfer coefficient, $m\ s^{-1}$ k_L: liquid phase mass transfer coefficient, $m\ s^{-1}$ k_G: gas phase mass transfer coefficient, $m\ s^{-1}$ k_m: membrane mass transfer coefficient, $m\ s^{-1}$ *l*: membrane thickness, m *L*: fibre length, m M_{CH4}: molecular weight of methane M_{gas}: molecular weight of the gas (air or N_2) *P*: gas side pressure, Pa r_p: membrane porous radius, m *T*: temperature, K β: empirical coefficient ε: membrane porosity ρ: density, $g\ m^{-3}$ μ: liquid or gas viscosity, $g\ m^{-1}\ s^{-1}$ *v*: liquid or gas velocity, $m\ s^{-1}$ μ: viscosity, $g\ m^{-1}\ s^{-1}$ ϕ: fibre packing fraction τ: membrane tortuosity Σv: special atomic diffusion volumes of the gas and methane, from [41]
Reynolds number, *Re*	$Re = \frac{d\,\rho\,v}{\mu}$	(7)	
Schmidt number, *Sc*	$Sc = \frac{\mu}{\rho\,D}$	(8)	
Graetz number, *Gz*	$Gz = \frac{d^2\,v}{D\,L}$	(9)	
Flow through the lumen			
Lévêque equation [34]	$Sh = 1.62\,Gz^{1/3}$ (for Gz>4)	(10)	
	$k_{L\ or\ G} = \frac{D}{d}\,1.62\left(\frac{d^2 v}{L\,D}\right)^{1/3}$	(11)	
Parallel flow through the shell			
Prasad and Sirkar (1988) [35]	$Sh = \beta\,\frac{d_e(1-\phi)}{L} Re^{0.6} Sc^{0.33}$	(12)	
	$k_{L\ or\ G} = D\,\beta\,\frac{(1-\phi)}{L}\left(\frac{d_e\,v\,\rho}{\mu}\right)^{0.6}\left(\frac{\mu}{\rho\,D}\right)^{0.33}$ for $0<Re<500$ and $0.04<\phi<400$ β=5.8 for hydrophobic membranes β=6.1 for hydrophilic membranes	(13)	
Dahuron and Cussler (1988) [36]	$Sh = 8\left(\frac{Re\,d_e}{L}\right) Sc^{0.33}$	(14)	
	$k_{L\ or\ G} = 8\,D\left(\frac{d_e v\,\rho}{\mu\,L}\right)\left(\frac{\mu}{\rho\,D}\right)^{0.33}$	(15)	
Porous Membrane			
Qi and Cussler (1985) [37]	$k_m = \frac{D_{G,eff}\,\varepsilon}{\tau\,l}$	(16)	
Kreulen et al (1993) [38]	$D_{G,eff} = \left(\frac{1}{D_{G,m}} + \frac{1}{D_{G,Kn}}\right)^{-1}$	(17)	
Fuller et al (1969) [41]	$D_{G,m} = \frac{0.01013\,T^{1.75}\left(\frac{1}{M_{gas}} + \frac{1}{M_{CH4}}\right)^{1/2}}{P\left[(\Sigma v)_{gas}^{1/3} + (\Sigma v)_{CH4}^{1/3}\right]^2}$	(18)	
Cussler (1984) [40]	$D_{G,Kn} = 97.0\,r_p\left(\frac{T}{M_{CH4}}\right)^{1/2}$	(19)	

Table 3. Diffusion coefficient of methane in water, nitrogen and air at 25 ºC and 1 bar.

Phase	Diffusion coefficient, D, $m^2\ s^{-1}$	Reference
Water	$1.76 \cdot 10^{-9}\ m^2\ s^{-1}$	[42]
Nitrogen	$2.19 \cdot 10^{-5}\ m^2\ s^{-1}$	[42]
Air	$1.76\ 10^{-5}\ m^2\ s^{-1}$	[41]

3. Results and discussion

3.1. Bioreactor start-up and operation: evolution of methane concentration in the system

The start-up of the bioreactor was carried out with a gradual increase in the organic loading rate (OLR) from 4 to 30 kg COD $m^{-3}\ d^{-1}$, resulting in six operating phases (from A to F, Table 4). Ethanol RE was higher than 97% from the beginning, and values of 99% were recorded after only 2 days of operation, which was maintained during the whole operation period. pH, alkalinity and VFA concentrations were monitored daily during the start-up (phase A to E), resulting in average value of 7.6 ± 0.2, 2788 ± 294 mg $CaCO_3\ L^{-1}$ and 13 ± 24 mg $CH_3COOH\ L^{-1}$, respectively. The high RE, stable pH and low VFA concentration indicated a smooth start-up of the reactor. Similar results were obtained during the operation at the maximum OLR of 30 kg COD $m^{-3}d^{-1}$ in phase F, in which the membrane contactor was connected for the removal of D-CH_4 from water. Average pH, alkalinity and VFA concentrations were 7.4 ± 0.2, 2821 ± 337 mg $CaCO_3\ L^{-1}$, and 51 ± 45 mg $CH_3COOH\ L^{-1}$, respectively. Similar results have been reported in previous experiments [27].

Methane content in the biogas generated in the reactor (%CH_4 exp.) was also monitored, and the results are presented in Table 4. Values were greater than 88% from phase A to E, higher than those estimated from stoichiometric ethanol anaerobic degradation (75% CH_4). This higher methane content is associated with the pH and bicarbonate alkalinity concentration in the system. From the experimentally measured pH, alkalinity and VFA concentrations, the theoretical methane content (%CH_4 est.) was estimated, assuming that CO_2 and CH_4 account for 100% of the biogas composition (measured H_2S concentration < 140 ppm) [43]. Equations used for estimation are included in Appendix A. The estimates are compared in Table 4 with the experimental results, and as can be seen, good agreement between estimated and experimental values was obtained, with relative errors lower than 3%.

D-CH_4 concentration in the water (C_{L1}, mg L^{-1}) was monitored, and results are shown in Table 4. The D-CH_4 concentration increased gradually with the OLR, so with biogas production. The methane oversaturation factor in water has been calculated as the ratio between the experimental and equilibrium D-CH_4 concentration with the gas phase (C_{L1}/C_{Leq}), and it has been included in the table. Equilibrium concentration of methane in the water of the bioreactor (C_{Leq}, mg L^{-1}) was calculated with the experimental methane content in the biogas (%CH_4 exp.) assuming a Henry's law constant of 29.55 for methane at 25 ºC [44]. In the first phase (A), D-CH_4 concentration was below the equilibrium value, but achieved values slightly higher than the equilibrium for phases between B and D (OLR = 9.2–20.0 kg COD $m^{-3}\ d^{-1}$). For OLR higher than 27 kg COD $m^{-3}\ d^{-1}$, the oversaturation factor showed values between 1.45 and 1.96. During phase F, when the membrane contactor was connected, the biogas generated had an average composition of 82 ± 3% CH_4, 18 ± 7% CO_2, and 110 ± 16 ppm H_2S. The average concentration of D-CH_4 in the water effluent entering the membrane contactor was 31.12 ± 3.1 mg L^{-1}. This value corresponded to an oversaturation factor of 1.72 ± 0.23. The methane oversaturation in

water effluents is frequently observed in laboratory and industrial bioreactors [45], and it could enhance the methane mass transfer coefficient in membrane contactors [9,12].

In Figure 2, the oversaturation factor is plotted against the daily methane production in the biogas (Q_{CH4}) for all the OLRs. A relationship can be inferred from the results, due to the increase in the D-CH_4 concentration with Q_{CH4}. The equilibrium D-CH_4 concentration (C_{Leq}) decreased slightly due to the decrease in $\%CH_{4exp}$ (from 17 to 21 mg D-CH_4 L^{-1}), which also had a positive effect in the oversaturation factor. However, the main parameter affecting the oversaturation is the increase in D-CH_4 concentration with the daily methane production.

Table 4. Methane content in the biogas ($\%CH_4$) and in the water effluent (C_{L1}) of the anaerobic reactor during the start-up (Phase A–E) and stable operation conditions (Phase F).

Phase (days)	OLR (kgCOD $m^{-3}d^{-1}$)	Day	pH	Alkalinity (mg $CaCO_3$ L^{-1})	Volatile fatty acids (mg CH_3COOH L^{-1}	$\%CH_4$ exp.	C_{L1} (mg CH_4 L^{-1})	Oversaturat. Factor (C_{L1}/C_{Leq})	$\%CH_4$ est.	Rel. Error (%)
A (0-6)	4.2±0.3	2	8.0± 0.1	2571±25	0	97±1	13.5±3.6	0.63	96	1.6
B (6-16)	9.2±0.9	9	7.6± 0.1	1351±36	0	95±1	25.1±0.7	1.19	94	0.8
		12	7.6± 0.2	2564±18	37±8	91±2	20.2±1.6	1.00	90	1.4
C (16-21)	11.7±0.2	16	7.6± 0.1	2762±12	41±6	90±2	20.6±0.9	1.03	89	1.6
		20	7.6± 0.1	1966±33	0	91±3	24.5±1.5	1.22	93	2.1
D (21-23)	20.0±0.4	22	7.5± 0.1	2872±41	0	88±1	20.5±1.3	1.05	85	3.0
E (23-29)	26.8±0.2	28	7.5± 0.1	2974±23	6±2	88±2	32.0±2.9	1.64	86	2.6
F (29-88)	30.2±0.5	48	7.5± 0.1	2944±25	42±7	84±2	27.0±0.6	1.45	86	1.9
		70	7.5± 0.2	3037±24	80±11	83±3	33.6±2.9	1.83	83	0.5
		73	7.5± 0.1	2832±11	127±16	83±2	30.2±2.7	1.63	86	2.7
		87	7.4± 0.2	3266±17	110±9	77±1	33.5±0.9	1.96	78	1.2

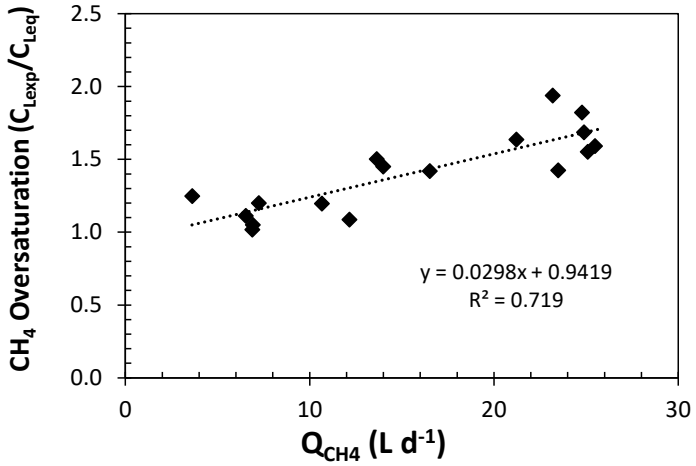

Figure 2. Variation of the oversaturation factor of methane in the anaerobic effluent with the daily methane production in the bioreactor

3.2. Parameters affecting the performance of the membrane contactor

Short-term experiments (time of operation ≤ 90 min) were carried out to characterize the performance of the PP membrane contactor both in the LS and SS mode at different operational conditions. Figure 3 shows the results as D-CH_4 RE versus liquid flow rate (Q_L) for the vacuum and sweep-gas operation. For the complete set of experiments, RE decreased with an increase in liquid flow rate, as frequently reported [9,11,12,14]. In the sweep-gas operation (Figure 3b), the decrease in RE was more pronounced when the liquid flowed in the lumen, with values ranging from around 98% to 67% for Q_L values between 4.1 and 27.2 L h^{-1}, respectively. When the N_2 flow rate was varied in the range 26–800 L N_2 h^{-1}, the performance of the system was unchanged and the RE nearly overlapped for all the liquid flow rates tested, suggesting that the gas phase mass transfer resistance was negligible. This indicates that the concentration of each transfer species in the gas phase was small enough to consider that the concentration in liquid phase in equilibrium with the gas phase was negligible compared to the actual concentration in the liquid phase ($C_L >> C_L^*$). In the vacuum operation (Figure 3a), for every liquid flow rate tested the RE increased with the increase in the vacuum applied, in the range from –140 to –800 mbar vacuum pressure (P_{vac}), suggesting that the concentration gradient (i.e. the driving force) increased with the P_{vac}, favoring D-CH_4 recovery. The maximum RE of 93% was achieved at the highest vacuum pressure (–800 mbar) and the lowest liquid flow rate (4.1 L h^{-1}) in lumen-side mode.

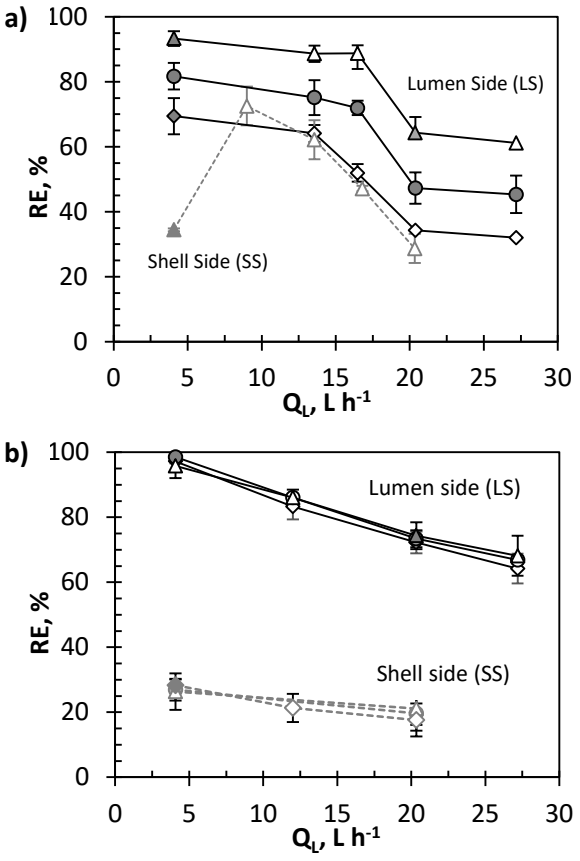

Figure 3. D-CH_4 removal efficiency versus liquid flow rate for the a) Vacuum operation (Δ –800 mbar; ○ –500 mbar; ◊ –140 mbar) and b) Sweep-gas operation (Δ 26, ○ 80 and ◊ 800 L N_2 h^{-1}). Filled gray symbols from Henares et al. [10].

Performance of the PP contactor in the operation with N_2 as sweep gas was similar to that observed with the maximum vacuum of –800 mbar when the liquid flowed through the lumen,

with the highest values of RE. However, behavior with the liquid in the shell differed considerably, and RE using sweep gas was considerable lower, especially at intermediate liquid flow rate (around 12 L h^{-1}), with a RE of 20% in sweep-gas mode and 60% in vacuum mode (–800 mbar). The singular low RE at Q_L of 4.1 L h^{-1} in the vacuum operation and SS mode (Figure 3a) could be associated with a high liquid mass transfer resistance at the lowest liquid flow rate due to poor shell-side distribution at low flow rates. Maldistribution of flow, the presence of stagnant zones, splitting and remixing of streams, and bypassing or channeling phenomena can occur more frequently in SS than in LS, and can be caused by the nonuniform fiber distribution and/or fiber deformation [3]. Although the Reynolds values are in the laminar range, localized turbulence or channeling around the fibers can lead to a higher dependence of the mass transfer coefficients on the Reynolds number than that typical of a laminar regime.

In the vacuum operation (Figure 3a), a sharp decrease in RE was observed for liquid flow rates higher than or equal to 13.6–16.5 L h^{-1} depending on pressure vacuum, a phenomenon attributed to the wetting of the pores that occurs when the pressure difference between liquid and gas side increases beyond the critical transmembrane pressure (TMP), phenomenon that will be discussed in the next section 3.3 in the mass transfer analysis. Because the diffusion coefficient of methane in liquid is much smaller than that in air (Table 3), the membrane transfer coefficient reduced remarkably when the membrane pores were penetrated by liquid, so the membrane mass transfer resistance increased as did the observed experimental resistance, which is depicted in Figure 4a1 against Q_L. The increase in pressure drop with the increase in the liquid velocity might be the reason for the appearance of wetting for flow rates higher than or equal to 13.6–16.5 L h^{-1}. Cui et al. [16] observed that the average membrane wetness and wetting rate grew with the increase in liquid velocity, and demonstrated that the TMP difference grew with an increase in the liquid flow rate, and this accelerates the movement of liquid into the membrane pores. Different authors have observed the increase in pore wetting with liquid velocity [10,16–18]. In the sweep operation, the wetting of the membrane seemed not to appear, probably due to the high pressure in the gas side that prevented the overcoming of the critical TMP. As a result, the experimental overall mass transfer resistance increased for the whole liquid flow-rate range (4b1 and 4b2). These observations are in agreement with the experimentally measured pressure drop in the contactor (Table 5). As expected, the increase in pressure drop with liquid velocity was observed, with a higher pressure drop in the LS mode than in the SS mode. However, in the LS mode, a sharp increase in the pressure drop was recorded for flow rates higher than 13.6 L h^{-1}. In the SS mode, the increase in the pressure drop was much more moderate, although an increase was also recorded from 20.4 L h^{-1}.

Table 5. Liquid pressure drop in the PP membrane contactor with the liquid flowing in the lumen (LS) and in the shell side (SS).

	Pressure drop[a], mbar	
Q_L, L h^{-1}	**Lumen Side**	**Shell side**
4.1	39	11
13.6	40	12
16.5	48	11
20.4	53	14
27.2	57	16

[a][10]

3.3. Mass transfer analysis

The experimental overall mass transfer coefficient (K_{Lexp}) of methane was calculated from the mass balance applied to the liquid phase in the contactor for all experiments (equation 4). Results are shown in Figure 4, expressed as the experimental mass transfer resistance ($R = (K_{Lexp}\ A_L)^{-1}$, with A_L value of 0.222 m^2 for lumen-side mode and 0.303 m^2 for shell-side mode). For the vacuum operation (Figure 4a1 and Figure 4a2), mass transfer resistance increased with the liquid flow rate in the range 13.6–20.4 L h^{-1} due the penetration of water into the pore structure (wetting operation), which resulted in the predominance of the membrane resistance in the system. Further increase in the liquid flow rate to 27 L h^{-1} promoted a decrease in the value of the overall resistance (for example from 3.20×10^5 to 2.70×10^5 s m^{-3}, at -140 mbar). Assuming that the individual membrane resistance at 27 L h^{-1} was equal or higher than at lower flow rates, this behavior is probably due to the rise in the individual liquid-side coefficient.

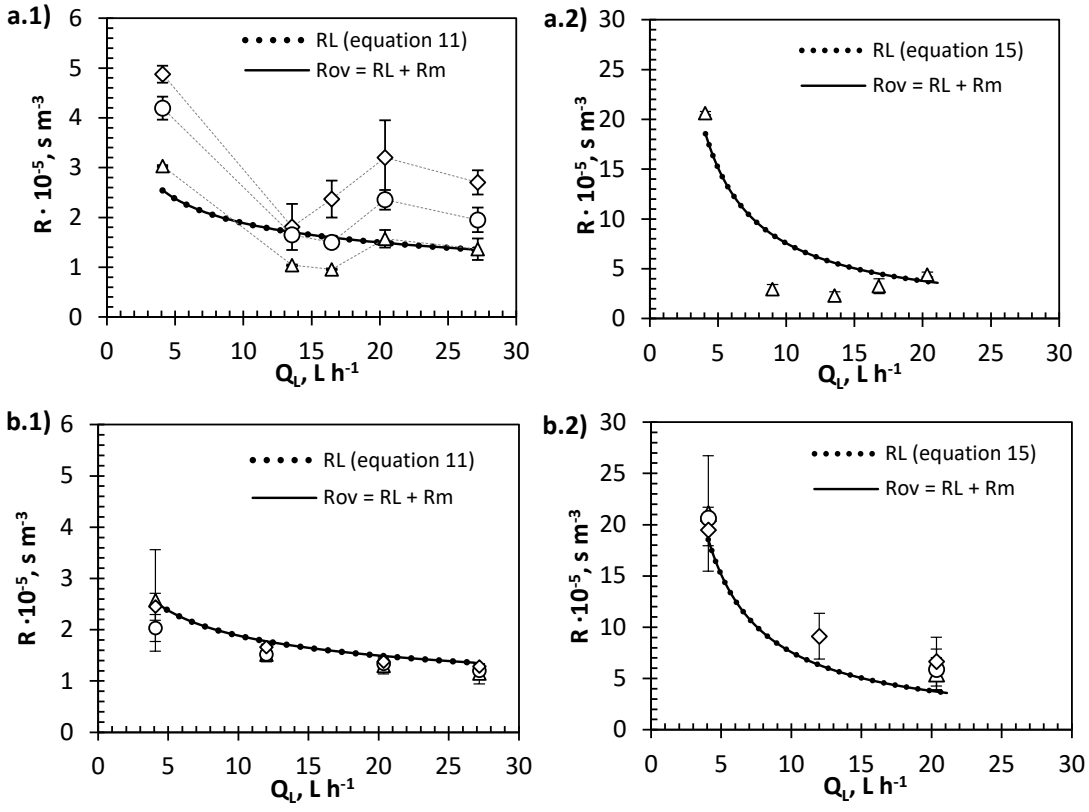

Figure 4. Comparison of the experimental (points) and estimated (lines) mass transfer resistance in different experiments. a) Vacuum experiments in lumen-side (1) and shell-side (2) mode (Δ – 800 mbar; ○ –500 mbar; ◊ –140 mbar). b) Sweep gas experiments in lumen-side (1) and shell-side (2) mode (Δ 26, ○ 80 and ◊ 800 L N_2 h^{-1}). [$R_L = (k_L A_L)^{-1}$; $R_m = (Hk_m A_{ml})^{-1}$; A_{ml} = 0.260 m^2, A_L(LS) = 0.222 m^2, A_L(SS) = 0.303 m^2)]

The overall mass transfer coefficients in the vacuum operation were calculated taking into account the concentration of methane in the gas side to estimate the equilibrium liquid concentration C_L^* (equation (4)). Methane concentration in the gas phase was assumed to be dependent of the gas pressure, since for every liquid flow rate the RE depended strongly on the vacuum pressure. Rongwong et al. [13] estimated the methane mole fraction in the gas outlet of a membrane contactor for different gas side pressures by a mathematical model, which included simultaneous methane and carbon dioxide desorption. The measured methane gas concentration

in our experiments at –500 mbar resulted in C_G = 74.76 ± 7.39 mg L^{-1}, which corresponded to a mole fraction of 0.23, very close to the estimate by Rongwong et al. (~0.22). This gas concentration corresponded to an equilibrium liquid concentration C_L^* of 2.53 mg L^{-1}. Thus, values for the pressures of –140 and –800 mbar were obtained from Rongwong et al. [13], estimates resulting in values of C_L^* of 5.82 and 0.51 mg L^{-1}, respectively, which correspond to methane mole fractions of ~0.30 and ~0.10. As a result, the experimental resistances values got closed (Figure 4a1), even though the effect of the vacuum pressure was still appreciable, especially for the highest vacuum (–800 mbar).

The experimental mass transfer coefficient in the sweep-gas operation was calculated assuming that the concentration of each transferred species in the gas phase was low enough to consider that C_L^* was negligible compared to the actual concentration in the liquid phase ($C_L >> C_L^*$; $C_L - C_L^* \sim C_L$). This assumption was supported experimentally, and it was corroborated by the performance results, since the RE nearly overlapped for different sweep gas flow rates (Figure 3b). The resulting mass transfer coefficients were similar to those reported in the literature. In this work, experimental coefficients ranged [1.94–3.74] $\times 10^{-5}$ m s^{-1} for liquid velocities between 0.013 and 0.086 m s^{-1} in lumen-side mode with sweep gas. Values of [2.5–3.2] $\times 10^{-5}$ m s^{-1} for velocities between 0.02 and 0.052 m s^{-1} were obtained with a polyvinylidene fluoride hydrophobically modified membrane [14]. With a commercial PP membrane similar to the one used in this study, values of [0.09–2.14] $\times 10^{-5}$ m s^{-1} for velocities between 0.0004 and 0.045 m s^{-1} were reported [11].

As expected, the experimental mass transfer resistance in the lumen-side flow was lower than in the shell-side flow. For the vacuum experiments, values ranged from 4.03 ± 0.93 × 10^5 to 1.50 ± 0.41 × 10^5 s m^{-3} (0.90 ± 0.21 × 10^5 to 0.33 ± 0.09 × 10^5 s m^{-1}) when liquid flows in the lumen-side were 4.1 and 13.6 L h^{-1}, respectively (Figure 4a1), and values ranged from 20.6 × 10^5 to 2.33 × 10^5 s m^{-3} (6.24 × 10^5 to 0.71 × 10^5 s m^{-1}) for the liquid in the shell side (Figure 4a2). For sweep-gas experiments, values ranged from 2.35 ± 0.28 × 10^5 to 1.21 ± 0.07 × 10^5 s m^{-3} (0.52 ± 0.06 × 10^5 to 0.27 ± 0.02 × 10^5 s m^{-1}) with liquid in the lumen at 4.1 and 27.2 L h^{-1}, respectively (Figure 4b1), and from 20.4 ± 0.8 × 10^5 to 5.99 ± 0.61 × 10^5 s m^{-3} (6.18 ± 0.25 × 10^5 to 1.81 ± 0.19 × 10^5 s m^{-1}) for the liquid in the shell side (Figure 4b2). Differences were due to the lower lumen cross-sectional area, which resulted in higher liquid velocities of the liquid in the lumen, so to a higher mass transfer coefficient. These differences were greater at low flow rates, indicating a power-law relation x^{-k} between resistance and liquid velocity.

Along with the experimental mass transfer resistance, the estimated resistance is depicted in Figure 4. The system can be described as the sum of the three serial resistances (equation 4): liquid, membrane and gas phases. Resistance of the gas side calculated with equations in Table 2 represented less than 7 × 10^{-3}% of the total resistance in the experiments using sweep gas and was considered negligible. In the experiments with the liquid in the lumen side, the gas resistance represented 1.4%, 1.0% and 0.5% of the total at vacuum pressures of –140, –500 and –800 mbar, respectively, and was also considered negligible for practical purposes.

The liquid phase mass transfer coefficient was estimated with the Lévêque solution (equation 11) for the experiments with lumen liquid flow (Figure 4a1 and Figure 4b1), and the resulting mass transfer resistance showed values between 2.54 × 10^5 and 1.35 × 10^5 s m^{-3} (0.56 × 10^5 and 0.30 × 10^5 s m^{-1}) for flow rates of between 4.1 and 27.1 L h^{-1}, respectively. As discussed before, this resistance ($R_L = (k_L A_L)^{-1}$) was predominant in the system and the overall resistance (R_{ov})

nearly matched that of the individual liquid phase. For the sweep-gas operation (Figure 4b1), the estimated resistance described quite accurately the experimental behavior (average relative error of 11.9 ± 7.0%), with a slight overestimate of the experimental resistance. For the vacuum operation (Figure 4a1), the estimated resistance was of the same order of magnitude as the experimental. At the lowest flow rate (4.1 L h^{-1}), the Lévêque equation underestimated the experimental resistances, which could suggest that gas-phase resistance might be playing an important role, especially at –140 and –500 mbar. At higher flow rates, the increase in the resistance due to the wetted operation prevented the fitting of the estimation without considering the increase in the membrane resistance due to pores being partially full of water.

Membrane resistance was estimated from the contributions of both molecular and Knudsen diffusion to the effective diffusion since pore radius was low enough to consider Knudsen diffusion (d < 0.1 μm). To include the wetting phenomena in the mass transfer analyses, a parameter x was considered, the pore fraction occupied by the liquid [17], and the membrane coefficient could then be estimated by:

$$\frac{1}{H \cdot k_m} = \frac{1}{H \cdot k_{m,G}}(1 - x) + \frac{1}{k_{m,L}}x \tag{20}$$

where $k_{m,G}$ and $k_{m,L}$ are the membrane transfer coefficients with the gas or liquid occupying the pores, respectively. $k_{m,G}$ is calculated by equation (16) and $k_{m,L}$ as follows:

$$k_{m,L} = \frac{D \cdot \varepsilon}{\tau \cdot l} \tag{21}$$

where D is the diffusion coefficient of methane in water (Table 3).

Estimated diffusion values are shown in Table 6 for the vacuum and sweep experiments, in which the resulting mass transfer coefficients and resistances are also included for dry (x = 0) and wetted operation (x≠0). In our system, the contribution of the Knudsen diffusion due to collisions of molecules with pore walls was greater than the molecular diffusion, and the resulting k_m values in dry conditions were in the range 4.28–5.52 × 10^{-2} m s^{-1}. As can be observed in Table 6, the estimated membrane resistance was five orders of magnitude lower than the experimental resistance when the pores were fully occupied by the gas phase (dry operation, x = 0). The presence of water in 25% of the membrane pores (x = 0.25) increased the resistance by five orders of magnitude, resulting in the same relevance as the liquid resistance. The increase in experimental resistance for flow rates higher than 16.5 L h^{-1} at –140 and –500 mbar of vacuum pressure and attributed to the wetting could be simulated by considering a pore fraction occupied by the liquid in the range 0.25–0.53. In Table 6, membrane resistance in the wetting mode with 25% (x = 0.25) and 53% (x = 0.53) of the pores occupied by the liquid is also included. Different authors have reported the impact of wetting in the permeate flux due to reduction of mass transfer. In the absorption of carbon dioxide in water using a PP membrane contactor similar to the one in this study, estimated liquid penetration lower than 13% resulted in a resistance of the liquid-filled pores accounting for over 98% of the membrane resistance and for 20–50% of the total resistance to absorption [17]. For the same application using commercial membrane contactors of PP and PVDF, the ratio of the membrane resistance increased sharply from 10 to 70% when only 10% of membrane length was wetted [18]. Values of wetting percentage of this work (25-53%) are higher than the reported values in the literature often around 10%, which could indicate that the equations employed overestimated the x value.

Table 6. Membrane mass transfer calculations: Molecular diffusion ($D_{G,m}$), Knudsen diffusion ($D_{G,Kn}$) and effective diffusion ($D_{G,eff}$) of methane in the membrane, and membrane mass transfer coefficient (k_m) and resistance (R_m) in dry (x = 0) and wetted (x≠0) conditions, for the vacuum and sweep-gas operations [$Rm = (Hk_mA_{ml})^{-1}$; $A_{ml} = 0.260\ m^2$].

	P_{vac}, mbar			Q_{N2}, L h^{-1}		
	–140	–500	–800	26	80	800
$D_{G,m}$, $m^2\ s^{-1}$	$2.45\cdot10^{-5}$	$4.16\cdot10^{-5}$	$1.00\cdot10^{-4}$	$2.20\cdot10^{-5}$	$2.19\cdot10^{-5}$	$2.10\cdot10^{-5}$
$D_{G,Kn}$, $m^2\ s^{-1}$	$8.37\cdot10^{-6}$	$8.37\cdot10^{-6}$	$8.37\cdot10^{-6}$	$8.37\cdot10^{-6}$	$8.37\cdot10^{-6}$	$8.37\cdot10^{-6}$
$D_{G,eff}$, $m^2\ s^{-1}$	$6.24\cdot10^{-6}$	$6.97\cdot10^{-6}$	$7.73\cdot10^{-6}$	$6.06\cdot10^{-6}$	$6.06\cdot10^{-6}$	$5.99\cdot10^{-6}$
k_m, m s^{-1} (x=0)	$4.45\cdot10^{-2}$	$4.98\cdot10^{-2}$	$5.52\cdot10^{-2}$	$4.33\cdot10^{-2}$	$4.33\cdot10^{-2}$	$4.28\cdot10^{-2}$
$R_m\ 10^{-5}$, s m^{-3} (x=0)	$2.92\cdot10^{-5}$	$2.61\cdot10^{-5}$	$2.35\cdot10^{-5}$	$3.00\cdot10^{-5}$	$3.00\cdot10^{-5}$	$3.04\cdot10^{-5}$
k_m, m s^{-1} (x=0.25)	$1.70\cdot10^{-6}$	$1.70\cdot10^{-6}$	$1.70\cdot10^{-6}$	---	---	---
$R_m\ 10^{-5}$, s m^{-3} (x=0.25)	0.76	0.76	0.76	---	---	---
k_m, m s^{-1} (x=0.53)	$8.03\cdot10^{-7}$	$8.03\cdot10^{-7}$	$8.03\cdot10^{-7}$	---	---	---
$R_m\ 10^{-5}$, s m^{-3} (x=0.53)	1.62	1.62	1.62	---	---	---

For the experiments with the liquid in the SS (Figure 4a2 and Figure 4b2), liquid mass transfer coefficient was estimated with equation (15) proposed by Dahuron and Cussler (1988) [36]. For the vacuum operation at –800 mbar (Figure 4a2), the calculated resistance overestimated the experimental at intermediate flow rates (9.0–13.6 L h^{-1}). For sweep-gas operation, the estimated resistance was slightly lower than the experimental, although acceptable agreement was observed considering the standard deviation of the results due to the low RE of shell-side/sweep-gas experiments. Equation (15) better fitted the experimental data than did equation (13), which could indicate the presence of channeling around the fibers in the shell-side mode.

3.4. Long-term operation: impact of fouling

Long-term stability of the membrane is of crucial interest for the final application of the technology since performance of membrane contactors can be adversely affected by wetting and/or fouling. Moreover, when coupling biological reactors and membrane technologies, flux decline due to fouling is one of the main drawbacks of membrane technology. Cleaning strategies might be optimized for the prevention of the use of cleaning chemicals to ensure an economically feasible operation with a long stable life of the system.

Experimental results of the long-term operation of the PP contactor in the LS and the SS mode are presented in Figure 5, as D-CH_4 RE versus time of operation, in which vertical lines indicate the application of the cleaning. In the LS mode (Figure 5a), a total of two operation/cleaning cycles were developed. In the first period, the RE was around 70% over 180 h of operation without any intermediate cleaning, demonstrating high stability performance of the system. A decrease in RE to 50% was recorded after 200 h, which was attributed to fouling of the membrane that included an additional mass transfer resistance. Two consecutive water cleanings of 0.5 and 2 h duration (Water Cleanings 1 and 2, respectively) only restored the initial RE during 50 h of operation (time of operation between Water cleaning 2 and Chemical Cleaning 1 in Figure 5). So, the chemical cleaning protocol was applied in two stages with NaOH (0.5 h)

and citric acid (0.5 h) in countercurrent flow (Chemical Cleaning 1). In this way, the initial RE of 70% was restored, as was the time of operation until the next decrease in RE (~200 h of operation). Again, after 590 h, a second chemical cleaning was necessary to recover the RE since Water Cleaning 3 did not succeed.

Different behavior was observed in SS mode (Figure 5b). The experiment was carried out with the same liquid flow rate as that in LS mode, resulting in a lower liquid velocity (0.017 m s^{-1} in SS and 0.065 m s^{-1} in LS). The initial RE of around 20% decreased to 10% after only 12 h of operation. This short operation time was attributed to a sudden increase in the suspended solids in the anaerobic effluent due to a partial disintegration of granules. The disintegration of granules in anaerobic reactors has been reported due to different factors such as sole carbon source, insufficient calcium supply, overloading or discontinuous substrate supply [28,46,47]. In our system, most of the disintegrated solids became trapped in the membrane prefilter; however, a small fraction entered the membrane contactor, being responsible for the blocking of some pores and the decrease in the RE. Again, Water Cleaning 1 of 2 h did not recover the performance, but the subsequent Chemical Cleaning 1 successfully restored the RE for 16 h of operation, the longest time of stable operation in continuous SS mode. Chemical Cleaning 2, carried out after 54 h of operation, increased the RE to the initial value (~20%), but the time of operation was slightly reduced to approximately 10 hours between Chemical Cleaning 2 and 3. Further Chemical Cleanings 3 and 4 with a total cleaning time of 6 h (3 h of NaOH + 3 h of citric acid) failed to restore the performance. This could be attributed to the presence of non-reversible fouling, and/or damage to the membrane material that could cause a change in the hydrophobicity. It is important to note that the time of operation without fouling was much lower in SS operation, probably due to the lower liquid velocity, which may favor the deposit of foulants from the biological reactor and promote the appearance of non-reversible fouling. We obtained similar results in the long-term operation of a PDMS membrane contactor for the demethanization of a similar anaerobic effluent [12]. This behaviour differs from the one observed in the filtration process of the membrane bioreactor (MBR) for water purification, in which deposits are brought to the membrane mainly by convective transport and the rate of fouling depends on velocity orthogonal to the surface (the permeate flux). In the membrane contactors for desorption of gases, the membrane acts as a physical support for the gas-liquid interface and the membrane keeps the two phases “in contact” without dispersing one phase into the other. For this particular membrane application, fluid mechanics are dominated by advection rather than convection (as with membrane filtration) thus the effects of concentration polarisation are limited [7].

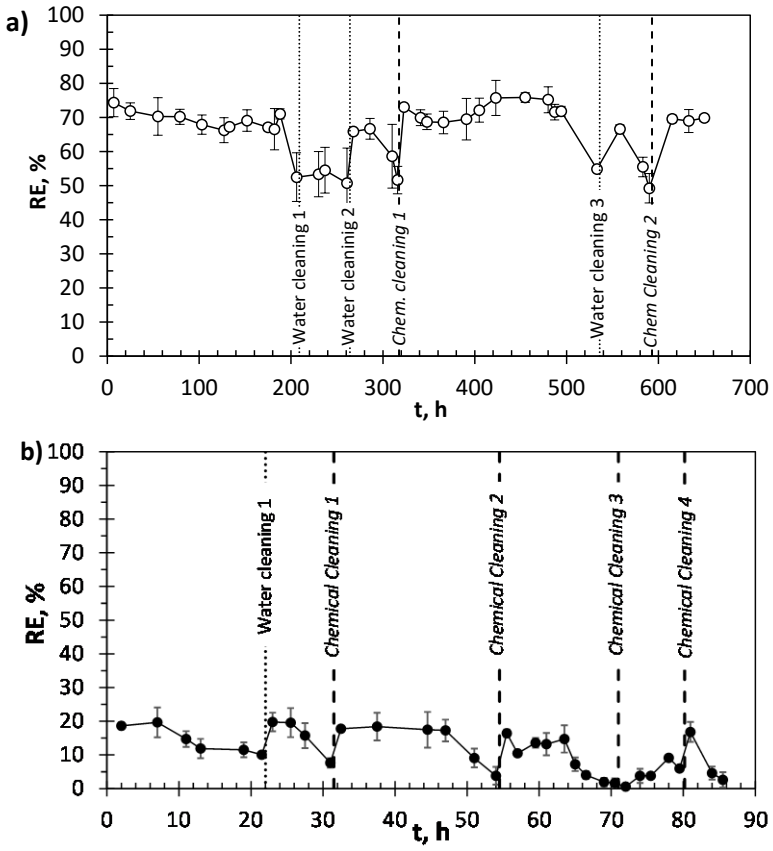

Figure 5. Performance of the membrane contactor in the long-term operation using N_2 as sweep gas (Q_L = 20 L h^{-1}; Q_{N2} = 26 L h^{-1}). a) Lumen-side mode, b) Shell-side mode.

Possible causes of loss of membrane performance in the long-term operation were investigated. Water samples from the inlet and outlet of the membrane contactor at different times of the long-term operation in LS and SS mode were analyzed, and the results are presented in Table 7, along with the results of the sample before the prefiltration. In the LS mode (Table 7a), the solid content did not change significantly after prefiltration. After the membrane, a decrease of 30% in volatile solids was detected, which could indicate the retention of organic matter in the membrane. In the SS mode, two samples were analyzed at different operation times. The first one corresponded to 21.5 h of operation, when the first decrease in RE was observed (Table 7b) and the degranulation episode occurred. In this case, suspended solid content (<0.7 μm) decreased slightly after prefiltration, but the solid content was not altered noticeably after the membrane contactor. The solid concentrations before prefiltration (i.e. the effluent of the bioreactor) were the highest of the three samples, confirming the increase in solid content of the effluent associated with the partial degranulation episode that caused the rapid loss of methane RE previously mentioned. In spite of the prefiltration of the anaerobic water, the solid concentration entering the membrane contactor was high at 21.5 hours of operation in shell side mode, which could cause the rapid loss of methane recovery efficiency (Figure 5b). The turbidity measurement decreased to a small extent in the outlet, indicating a slight retention of particulate matter. We obtained similar results in our previous work, with a reduction of proteins and turbidity at the outlet of a PDMS membrane contactor [12]. The VFAs present in the inlet of the membrane contactor were practically eliminated, probably removed by sweep gas along with CH_4 and CO_2. The reduction in soluble COD may also indicate that ethanol in the inlet of the contactor was partially removed. Soluble polysaccharide content increased

significantly after filtration, indicating that some extracellular polymeric substances could be retained in the filter, and highlighting the importance of regular filter maintenance. The water characterization after 44.5 h of operation confirmed the results previously observed. No water parameter changed significantly after the membrane contactor, except the VFA and COD concentrations. Moreover, analysis of anions (Cl^-, NO_3^-, SO_4^{2-}, PO_4^{3-}) and cations (Na^+, NH_4^+, K^+, Ca^{2+} and Mg^{2+}) concentrations were carried out in order to elucidate the inorganic fouling, and results did not show significant differences between the samples (results not shown).

Table 7. Water characterization before the prefilter (Prefilter), at the membrane inlet (Pre-membrane) and at the membrane outlet (Post-membrane) in the long-term experiments. a) Lumen-side mode after 650 h, b) Shell-side mode after 21 h, and c) Shell-side mode after 44 h.

a) Lumen side operation (Sampling at t = 650 h – RE = 70%)			
	Pre-filter	**Pre-membrane**	**Post-membrane**
TS (mg L^{-1})	3810 ± 61	3903 ± 66	3777 ± 6
VS (mg L^{-1})	230 ± 8	263 ± 28	160 ± 12
SS (mg L^{-1})	37 ± 12	35 ± 1	37 ± 1
VSS (mg L^{-1})	37 ± 12	30 ± 2	31 ± 4
b) Shell side operation (Sampling at t = 21.5 h – RE = 10%)			
	Pre-filter	**Pre-membrane**	**Post-membrane**
TS (mg L^{-1})	4340 ± 598	4146 ± 461	4280 ± 587
VS (mg L^{-1})	716 ± 28	665 ± 41	770 ± 74
SS (mg L^{-1})	112 ± 34	80 ± 24	76 ± 11
VSS (mg L^{-1})	96 ± 10	74 ± 3	74 ± 3
Turbidity (NTU)	85	83	68
VFA (mg CH_3COOH L^{-1})	6	6	<LoD*
COD (mg L^{-1})	65 ± 5	67 ± 5	44± 2
Polysaccharides, mg L^{-1}	3.7 ± 0.1	7.4 ± 0.2	8.1 ± 0.4
Proteins, mg L^{-1}	---	---	---
c) Shell side operation (Sampling at t = 44.5 h – RE = 18%)			
	Pre-filter	**Pre-membrane**	**Post-membrane**
TS (mg L^{-1})	3355 ± 598	3432 ± 461	3516 ± 587
VS (mg L^{-1})	161 ± 15	148 ± 11	149 ± 22
SS (mg L^{-1})	120 ± 24	50 ± 18	56 ± 9
VSS (mg L^{-1})	118± 12	48 ± 6	50 ± 9
Turbidity (NTU)	27	24	25
VFA (mg CH_3COOH L^{-1})	112	48	5
COD (mg L^{-1})	62 ± 6	64 ± 6	40 ± 2
Polysaccharides, mg L^{-1}	5.3 ± 2.4	5.6 ± 1.2	6.2 ± 0.7
Proteins, mg L^{-1}	3.8 ± 0.3	10.2 ± 0.1	11.2 ± 0.2
**LoD: Limit of Detection*			

The cleaning effluents of Chemical Cleaning 3 of the experiments in SS mode were also completely characterized. The chemical cleaning consisted of 2 h cleaning with 2 L of NaOH followed by 2 h cleaning with 2 L citric acid with continuous recirculation of the solutions. In this case, the cleaning solutions were divided into four aliquots of 0.5 L, recirculated for 0.5 h

and then analyzed. Results of the parameters showing important variations are presented in Figure 6. Results showed an increase in concentration of suspended solids (SS) in the NaOH solution, which were mainly inorganic (25% volatile suspended solids, VSS) (Figure 6a). The highest concentration was recorded after 0.5 h of cleaning, with a smooth decrease until values higher than the initial solution concentration. The peak of suspended solids was accompanied by an increase in turbidity. The citric acid solution removed a much greater quantity of suspended solids, but in this case mainly organic (99% VSS). In this case, turbidity measurements were very low. Again, a high peak of around 900 mg VSS L^{-1} was observed after 0.5 h, and the suspended solid concentration remained at a high value of around 380 mg SS L^{-1} after 2 h cleaning. Regarding the soluble fraction, NaOH cleaning also cleaned out polysaccharides and proteins, suggesting the presence on the membrane surface of extracellular polymeric substances and other organic foulants generated from the cellular lysis inside the bioreactor, which could be the cause of the loss of efficiency. After 2 hours of cleaning, concentration of polysaccharides in the NaOH solution was of 8 mg L^{-1}, higher than the concentration of the initial solution (< 2 mg L^{-1}) (Figure 6b). These results suggested that the cleaning did not remove completely the organic foulants attached to the membrane, and this may be the cause of the rapid loss of performance after this cleaning. Thus, a new chemical cleaning (number 4) was carried out but the performance did not recover, confirming the presence of non-reversible fouling.

Even though the analyses of water samples during the long-term operation did not show any significant variation to explain the nature of the fouling, cleaning solution analysis revealed that fouling could be associated with both organic and inorganic foulants. NaOH solution washed out inorganic solids, polysaccharides and proteins, whereas citric acid solution washed out a large quantity of organic solids. A higher concentration of organic foulants were washed out, confirming that the fouling was characterized mainly by extracellular polymeric substances and other biofoulants coming from the anaerobic reactor.

The analyses of water at the inlet and outlet of the contactor during the long-term experiments did not provide conclusive results about the nature of the fouling, probably due to the low variation of some parameters along with the low accuracy of some analytical methods. Instead, follow-up on the concentration of potential foulants in the cleaning solutions is recommended as an experimental protocol, not only to elucidate the character of the fouling but also to optimize the cleaning procedure.

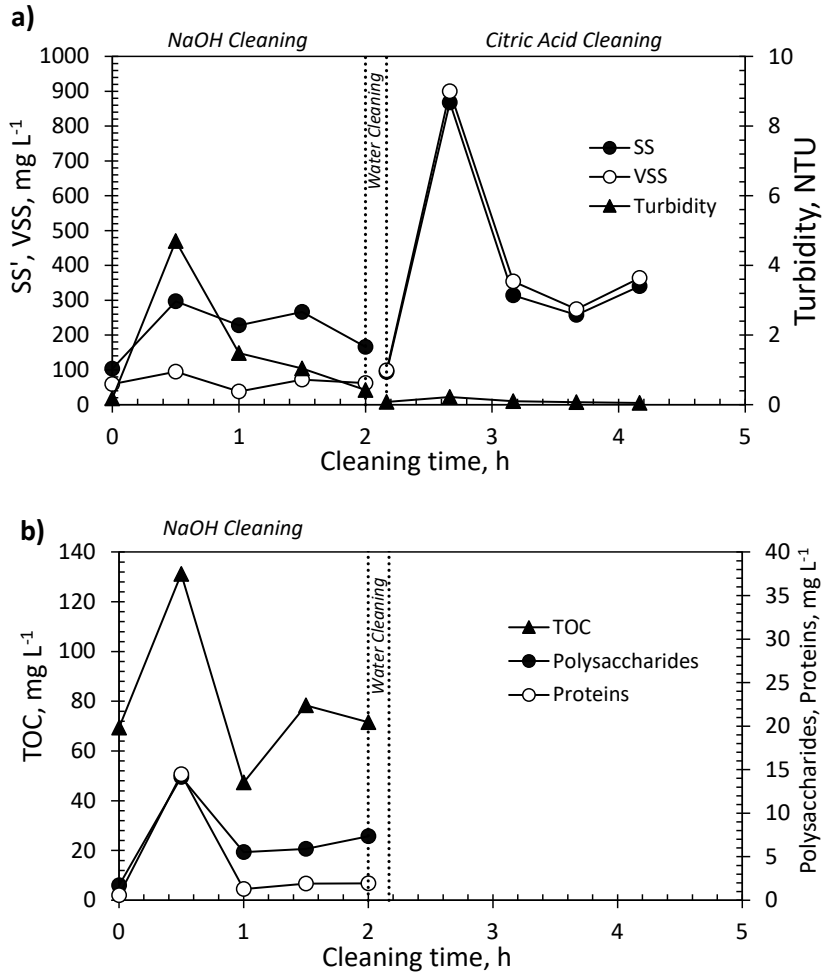

Figure 6. Results of the characterization of NaOH and citric acid cleaning solutions with time of Chemical Cleaning 3 of the long-term experiment in shell-side mode: a) Suspended Solids (SS), Volatile Suspended Solids (VSS), Turbidity; b) Soluble Total Organic Carbon (TOC), polysaccharides and proteins.

An additional experiment was carried out to confirm the presence of biofouling. A solution of similar composition to the feed of the anaerobic reactor (i.e. ethanol as organic substrate and a mixture of nutrients) was fed into the membrane contactor in a closed loop over 4 h with no sweep gas or vacuum pressure. Concentration of ethanol at the beginning and end of the test was measured as TOC concentration. A blank test with the membrane after chemical cleaning resulted in an ethanol removal of 5%, which can be explained by ethanol evaporation or transference to the gas phase. The same assay in the presence of confirmed fouling (before cleaning) resulted in a considerably higher ethanol removal of 28%. In the absence of sweep gas and vacuum, this could indicate that ethanol biodegradation occurred to some extent inside the contactor affected by fouling, suggesting the presence of biological degrading activity and hence the biofouling. Although also physical or chemical sorption of ethanol onto the inorganic and/or organic foulants could be involved in the ethanol depletion, previous studies suggest that most of the biomass and potential inorganic deposits have affinity to water in ethanol/water

mixtures and almost no ethanol might be adsorbed [48,49]. Further investigation in fouling characterization is necessary to elucidate the predominant mechanisms.

Results demonstrate that a cleaning strategy to prevent operational failure due to fouling is necessary. During the short-term experiments, a daily cleaning with deionized water in countercurrent flow for 30 min was applied. This water backwash cleaning method was found to maintain the methane RE over 3510 h of operation in LS mode and 1620 h in SS mode without fouling [28]. Since this method does not require chemicals (i.e. does not cause secondary pollution), is cost-saving and is easy to perform, it would be recommended as the regular cleaning method.

4. Conclusions

The use of a PP membrane contactor for the recovery of dissolved methane from anaerobic effluents has been demonstrated as an efficient and promising technology. Higher removal efficiencies can be obtained using vacuum pressure or sweep gas in the gas side, and good performance in long-term operation may be achieved by prefiltration of the effluent for particulate matter removal and by using a preventive cleaning based on a daily water countercurrent wash-out.

In the vacuum operation, pore wetting was detected when increasing the liquid flow rate at intermediate values, probably due to the increase in the pressure drop. The liquid mass transfer resistance was the most relevant in the system, especially during the dry operation (non-wetted mode). As expected, the membrane resistance gained importance in the wetted operation, and an estimated wet pore fraction of between 0.25 and 0.53 could simulate the experimental results in the wetted operation. The use of nitrogen as sweep gas resulted in a more efficient and stable operation. Higher removal efficiencies were obtained in lumen-side mode, and pore wetting was not detected, probably due to the lower TMP. No influence of the gas flow rate was observed.

Long-term operation was performed in the lumen-side and shell-side modes with the same liquid flow rate. Higher operation time in lumen-side mode was observed, of 180 h, against 16 h in shell-side mode. Water cleaning was not effective when fouling had already affected the RE, and chemical cleanings were necessary to restore the performance. Analyses of cleaning samples for characterization of the shell-side fouling revealed that volatile and non-volatile suspended solids were washed out. Polysaccharides and proteins were also cleaned out from the membrane contactor, suggesting the presence of extracellular polymeric substances. Thus, the presence of both inorganic and organic foulants seemed to be responsible for the performance decline. Ethanol biodegradation in the membrane contactor was suggested, and hence the biological nature of the fouling. Based on experimental results of the short-term experiments, a daily water cleaning of 30 min is proposed to prevent fouling and to extend the operational life.

Acknowledgments

Financial support was obtained from the Ministerio de Economía y Competitividad (Spain, project CTM-2014–54517-R, co-financed by FEDER funds). M. Henares acknowledges Generalitat Valenciana for financial support for her PhD (Spain, Prometeo project 2013/53). The authors wish to thank Marta Bofi for her support in the experimental work.

References

[1] S.H. Yalkowsky, Y. He, P. Jain, Handbook of Aqueous Solubility Data, 2nd ed., CRC Press, Taylor&Francis, Florida, 2010.

[2] S. Heile, C.A.L. Chernicharo, E.M.F. Brandt, E.J. McAdam, Dissolved gas separation for engineered anaerobic wastewater systems, Sep. Purif. Technol. 189 (2017) 405–418.

[3] E. Drioli, A. Criscuoli, E. Curcio, Membrane Contactors: Fundamentals, Applications and Potentialities,Volumen 11, 1st ed., Elsevier Science, Amsterdam, 2005.

[4] T.A. Cramer, D.W. Johnson, M.A. Urynowicz, Membrane gas transfer of methane and carbon dioxide in submerged coal deposits, Environ. Technol. 30 (2009) 11–20.

[5] W.M.K.R.T.W. Bandara, H. Satoh, M. Sasakawa, Y. Nakahara, M. Takahashi, S. Okabe, Removal of residual dissolved methane gas in an upflow anaerobic sludge blanket reactor treating low-strength wastewater at low temperature with degassing membrane, Water Res. 45 (2011) 3533–3540.

[6] W.M.K.R.T.W. Bandara, T. Kindaichi, H. Satoh, M. Sasakawa, Y. Nakahara, M. Takahashi, S. Okabe, Anaerobic treatment of municipal wastewater at ambient temperature: Analysis of archaeal community structure and recovery of dissolved methane., Water Res. 46 (2012) 5756–64.

[7] J. Cookney, E. Cartmell, B. Jefferson, E.J. McAdam, Recovery of methane from anaerobic process effluent using poly-di-methyl-siloxane membrane contactors., Water Sci. Technol. 65 (2012) 604–10.

[8] G. Luo, W. Wang, I. Angelidaki, A new degassing membrane coupled upflow anaerobic sludge blanket (UASB) reactor to achieve in-situ biogas upgrading and recovery of dissolved CH_4 from the anaerobic effluent, Appl. Energy. 132 (2014) 536–542.

[9] J. Cookney, A. Mcleod, V. Mathioudakis, P. Ncube, A. Soares, B. Jefferson, E.J. McAdam, Dissolved methane recovery from anaerobic effluents using hollow fibre membrane contactors, J. Memb. Sci. 502 (2016) 141–150.

[10] M. Henares, M. Izquierdo, J.M. Penya-Roja, V. Martínez-Soria, Comparative study of degassing membrane modules for the removal of methane from Expanded Granular Sludge Bed anaerobic reactor effluent, Sep. Purif. Technol. 170 (2016) 22–29.

[11] A. McLeod, B. Jefferson, E.J. McAdam, Toward gas-phase controlled mass transfer in micro-porous membrane contactors for recovery and concentration of dissolved methane in the gas phase, J. Memb. Sci. 510 (2016) 466–471.

[12] M. Henares, M. Izquierdo, P. Marzal, V. Martínez-Soria, Demethanization of aqueous anaerobic effluents using a polydimethylsiloxane membrane module: Mass transfer, fouling and energy analysis, Sep. Purif. Technol. 186 (2017).

[13] W. Rongwong, S. Wongchitphimon, K. Goh, R. Wang, T.-H. Bae, Transport properties of CO_2 and CH_4 in hollow fiber membrane contactor for the recovery of biogas from anaerobic membrane bioreactor effluent, J. Memb. Sci. 541 (2017) 62–72.

[14] G.S.M.D.P. Sethunga, W. Rongwong, R. Wang, T.-H. Bae, Optimization of hydrophobic modification parameters of microporous polyvinylidene fluoride hollow-fiber membrane for biogas recovery from anaerobic membrane bioreactor effluent, J. Memb. Sci. 548 (2018) 510–518.

[15] W. Rongwong, R. Jiraratananon, S. Atchariyawut, Experimental study on membrane wetting in gas-liquid membrane contacting process for CO2 absorption by single and mixed absorbents, Sep. Purif. Technol. 69 (2009) 118–125.

[16] L. Cui, Z. Ding, L. Liu, Y. Li, Modelling and Experimental Study of Membrane Wetting in Microporous Hollow Fiber Membrane Contactors, Can. J. Chem. Eng. 93 (2015) 1254–1265.

[17] M. Mavroudi, S.P. Kaldis, G.P. Sakellaropoulos, A study of mass transfer resistance in membrane gas-liquid contacting processes, J. Memb. Sci. 272 (2006) 103–115.

[18] H.Y. Zhang, R. Wang, D.T. Liang, J.H. Tay, Theoretical and experimental studies of membrane wetting in the membrane gas-liquid contacting process for CO2 absorption, J. Memb. Sci. 308 (2008) 162–170.

[19] Z. Cui, D. deMontigny, Experimental study of carbon dioxide absorption into aqueous ammonia with a hollow fiber membrane contactor, J. Memb. Sci. 540 (2017) 297–306.

[20] A. Malek, K. Li, W.K. Teo, Modeling of Microporous Hollow Fiber Membrane Modules Operated under Partially Wetted Conditions, Ind. Eng. Chem. Res. 36 (1997) 784–793.

[21] S. Micropower Europe, C.T. Corporation, Microturbines specifications - Brochure, (2018). http://www.micropowereurope.com/Inicio/index.php/ (accessed February 22, 2018).

[22] C. Vallieres, E. Favre, Vacuum versus sweeping gas operation for binary mixtures separation by dense membrane processes, J. Memb. Sci. 244 (2004) 17–23.

[23] X. Shi, G. Tal, N.P. Hankins, V. Gitis, Fouling and cleaning of ultrafiltration membranes: A review, J. Water Process Eng. 1 (2014) 121–138.

[24] P. Ferrero, P. San-Valero, C. Gabaldón, V. Martínez-Soria, J.M. Penya-roja., Anaerobic degradation of glycol ether-ethanol mixtures using EGSB and hybrid reactors: performance comparison and ether cleavage pathway, J. Environ. Manag. 213 (2018) 159–167.

[25] R. Klaassen, P.H.M. Feron, A.E. Jansen, Membrane contactors in industrial applications, Chem. Eng. Res. Des. 83 (2005) 234–246.

[26] R. Chan, V. Chen, Characterization of protein fouling on membranes: Opportunities and challenges, J. Memb. Sci. 242 (2004) 169–188.

[27] L.S. Clesceri, A.D. Eaton, A.E. Greenberg, M.A.H. Franson, eds., Standard methods for the examination of water and wastewater, 22nd ed., American Public Health, Washington DC, 2012.

[28] C. Lafita, J.M. Penya-roja, C. Gabaldón, Anaerobic removal of 1-methoxy-2-propanol under ambient temperature in an EGSB reactor, Bioprocess Biosyst. Eng. (2015) 2137–2146.

[29] M. Henares, Recuperación de metano disuelto en el efluente de un reactor anaerobio de lecho expandido mediante contactores de membrana, PhD Thesis, Universitat de València, 2017. http://roderic.uv.es/handle/10550/59057 (accessed 10 March 2018).

[30] 3M Company, Cleaning Guidelines of Liqui-Cell Membrane Contactors, (2016). http://www.liquicel.com/technical-resources/startup-operating-guides.cfm (accessed March 16, 2018).

[31] M. Dubois, K.. Gilles, K. Hamilton, J, P. Rerbers, F. Smith, Colorimetric method for determination of sugars and related substances., Anal. Chem. 28 (1956) 350–356.

[32] O.H. Lowry, N.J. Rosebrough, L.A. Farr, R.J. Randall, Protein measurement with the folin phenol reagent, J. Biol. Chem. 193 (1951) 265–275.

[33] A. Gabelman, S. Hwang, Hollow fiber membrane contactors, J. Memb. Sci. 159 (1999) 61–106.

[34] M.A. Lévêque, Les lois de la transmission de chaleur par convection, Les Ann. Des Mines. 13 (1928) 201–299.

[35] R. Prasad, K. Sirkar, Dispersion-free solvent extraction with microporous hollow fiber modules, AIChE J. 34 (1988) 177–188.

[36] L. Dahuron, L. Cussler, Protein Extractions with Hollow Fibers, AIChE J. 34 (1988) 131–136.

[37] Z. Qi, E.L. Cussler, Microporous hollow fibers for gas absorption. II. Mass transfer across the membrane., J. Memb. Sci. 23 (1985) 321–332.

[38] H. Kreulen, C.A. Smolders, W.P.M.V.A.N. Swaaij, Determintation of mass transfer rates in wetted and non-wetted microporous membranes, Chem. Eng. Sci. 48 (1993).

[39] E.N. Fuller, K. Ensley, J.C. Giddings, Diffusion of halogenated hydrocarbons in helium. The effect of structure on collision cross sections, J. Phys. Chem. 73 (1969) 3679–3685.

[40] E.L. Cussler, Diffusion: Mass Transfer in Fluid Systems, Cambridge University Press, 1984.

[41] E.N. Fuller, P.D. Schettler, J.C. Giddings, A new method for prediction of binary gas-phase diffusion coefficients, Ind. Eng. Chem. 58 (1966) 18–27.

[42] Y. Cengel, M. Boles, Thermodynamics:An Engineering Approach, 6th ed., McGraw-Hill, New York, 2008.

[43] J. Grady, G.T. Daigger, N.G. Love, C.D.M. Filipe, Biological wastewater treatment, 3rd ed., Taylor&Francis, New York, 2011.

[44] R. Sander, Compilation of Henry's law constants (version 4.0) for water as solvent, Atmos. Chem. Phys. 15 (2015) 4399–4981.

[45] B.C. Crone, J.L. Garland, G.A. Sorial, L.M. Vane, Significance of dissolved methane in effluents of anaerobically treated low strength wastewater and potential for recovery as an energy product: A review, Water Res. 104 (2016) 520–531.

[46] X. Lu, G. Zhen, M. Chen, K. Kubota, Y. Li, Biocatalysis conversion of methanol to methane in an upflow anaerobic sludge blanket (UASB) reactor: Long-term performance and inherent deficiencies, Bioresour. Technol. 198 (2015) 691–700.

[47] K. Torres, F.J. Álvarez-Hornos, P. San-Valero, C. Gabaldón, P. Marzal, Granulation and microbial community dynamics in the chitosan-supplemented anaerobic treatment of wastewater polluted with organic solvents, Water Res. 130 (2018) 376–387.

[48] K.E. Beery, M.R. Ladisch, Adsorption of Water from Liquid-Phase Ethanol-Water Mixtures at Room Temperature Using Starch-Based Adsorbents, Ind. Eng. Chem. Res. 40 (2001) 2112-2115.

[49] A. Al-Asheh, F. Banat, N. Al-Lagtah, separation of ethanol–water mixtures using molecular sieves and biobased adsorbents, Chem. Eng. Res. Des., 82 (2004) 855–864